

# Research on Measurement Accuracy of Laser Tracking System Based on Spherical Mirror with Rotation Errors of Gimbal Mount Axes

Zhaoyao Shi, Huixu Song, Hongfang Chen, Yanqiang Sun

*Beijing Engineering Research Center of Precision Measurement Technology & Instruments, Beijing University of Technology, No.100, Pingleyuan, Chaoyang District, 100124, Beijing, China, shizhaoyao@bjut.edu.cn*

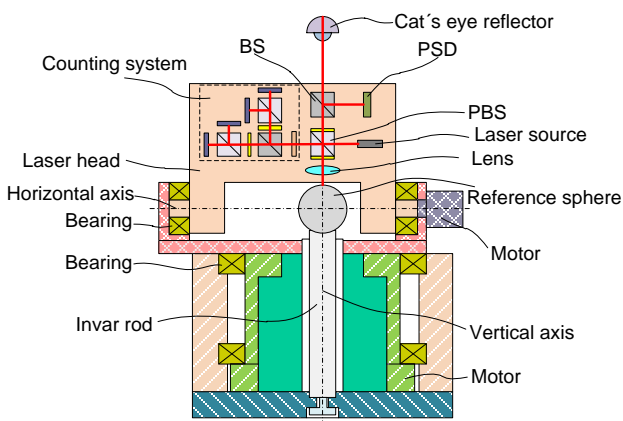
This paper presents a novel experimental approach for confirming that spherical mirror of a laser tracking system can reduce the influences of rotation errors of gimbal mount axes on the measurement accuracy. By simplifying the optical system model of laser tracking system based on spherical mirror, we can easily extract the laser ranging measurement error caused by rotation errors of gimbal mount axes with the positions of spherical mirror, biconvex lens, cat's eye reflector, and measuring beam. The motions of polarization beam splitter and biconvex lens along the optical axis and vertical direction of optical axis are driven by error motions of gimbal mount axes. In order to simplify the experimental process, the motion of biconvex lens is substituted by the motion of spherical mirror according to the principle of relative motion. The laser ranging measurement error caused by the rotation errors of gimbal mount axes could be recorded in the readings of laser interferometer. The experimental results showed that the laser ranging measurement error caused by rotation errors was less than  $0.1 \mu\text{m}$  if radial error motion and axial error motion were within  $\pm 10 \mu\text{m}$ . The experimental method simplified the experimental procedure and the spherical mirror could reduce the influences of rotation errors of gimbal mount axes on the measurement accuracy of the laser tracking system.

Keywords: Spherical mirror, laser tracking system, gimbal mount axes, rotation errors, relative motion thinking.

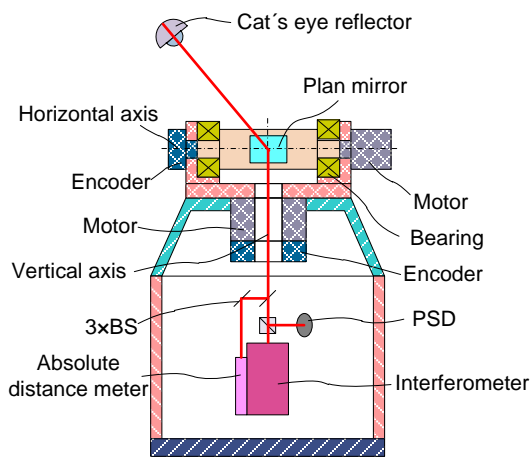
## 1. INTRODUCTION

Laser tracking system is a large-scale measurement system with high precision in industrial measurement fields, and is similar to a portable coordinate measuring system (PCMS). It is widely applied in shipbuilding, automobile manufacturing, and aircraft manufacturing with requirements of large measuring scale, high measuring efficiency, high measuring precision and simple operation [1]. Rotational motion unit plays an indispensable role in the laser tracking system, and it is also the basic unit for the motions of tracking. However, rotation errors of rotational motion unit may decrease the measurement accuracy of the laser tracking system. Therefore, a special shafting structure can decrease the influences of rotation errors on the outcome of sensors in the laser tracking system and improve the measurement accuracy [2]-[3]. As shown in Fig.1.a), LaserTracer, which holds a stable optical reference sphere as reflection unit, has been developed by English and German national metrology institutes, the NPL and the PTB, and Etalon AG [4]-[7]. Its special shafting structure is named gimbal mount axes (vertical axis and horizontal axis). Laser head, which contains all the optical components as a whole, is driven by gimbal mount axes. As the reflection unit, the reference sphere is mounted on an invar rod that passes

through a hollow shaft and is fixed on the bottom of equipment. The position of the reference sphere does not change with the motion of gimbal mount axes. The reference sphere in LaserTracer also possesses a perfect form, with the form error less than 50 nm. In this design, Laser Tracer not only possesses the large measuring angle, but also minimizes the influences of rotation errors on the laser ranging measurement accuracy [8]. As shown in Fig.1.b), in traditional commercial laser trackers, a plan mirror is fixed at the intersection of two axes as the reflection unit inside the instrument to reflect laser beam and the intersection serves as the origin under the spherical coordinate system defined by laser tracker. Laser beam from the instrument points to the origin and is reflected to the measurement space by the mirror [1], [9]. Due to the direct contact with two axes, the position of the mirror is changed by rotation error motions of two axes. The position of laser spot and the angle between laser beam and optical axis are also correspondingly changed, so a traditional commercial laser tracker can hardly avoid the influences of rotation error motions caused by vibration and motility of axes [10]-[11]. The measurement accuracy of the laser tracker is decreased because the measurement error caused by vibration and motility of axes can hardly be compensated [12]-[13].



a) Basic structure of LaserTracer.



b) Basic structure of Laser Tracker.

Fig.1. Basic structures of two kinds of laser tracking systems.

Up to now, only LaserTracer has used this structure to reduce the influences of rotation errors of gimbal mount axes. However, the characteristic of this structure has not been deeply explored. This paper presents a simplified experimental approach for confirming that the spherical mirror of the laser tracking system can reduce the influences of rotation errors of gimbal mount axes on the measurement accuracy.

2. SUBJECT & METHODS

2.1. Rotation errors in LaserTracer

Interferometer integrated in the laser head of LaserTracer measures the relative displacement from the center of the reference sphere to the center of the cat's eye reflector in 3-D space (Fig.1.a)) [14]. The center of the reference sphere, which is also the intersection point between gimbal mount axes and laser beam, serves as the origin of LaserTracer. The four-way electrical signals emitted by quadrant detector are used to control vertical and horizontal axes so that the laser beam points to the center of the cat's eye reflector and PSD. However, when LaserTracer is tracking the cat's eye

reflector, laser spot moves in an irregular direction on the surface of the reference sphere due to the rotation errors (Fig.2.). There are 6 rotation errors for each axis [15]-[16]. The total 12 rotation errors for horizontal axis and vertical axis can be considered as two movements for the laser head because the laser head is connected with gimbal mount axes. The error motions caused by rotation errors can be divided into error motion along the vertical direction of measuring beam and error motion along the direction of measuring beam. The two kinds of error motions should be within the range of  $\pm 20 \mu\text{m}$ .

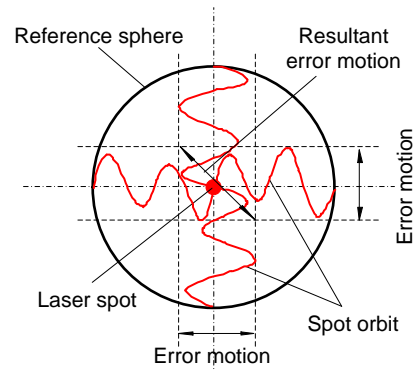


Fig.2. Laser spot orbit on the surface of the reference sphere.

The optical system of LaserTracer is shown in Fig.3. Laser beam from optical fiber passes through the polarization beam splitter (PBS) and is then separated into two parts (polarized beams P and S). Polarized beam P enters the counting system as the reference beam, whereas polarized beam S reflected by PBS, the cat's eye reflector and reference sphere interfere with the reference beam in counting system as measuring beam.

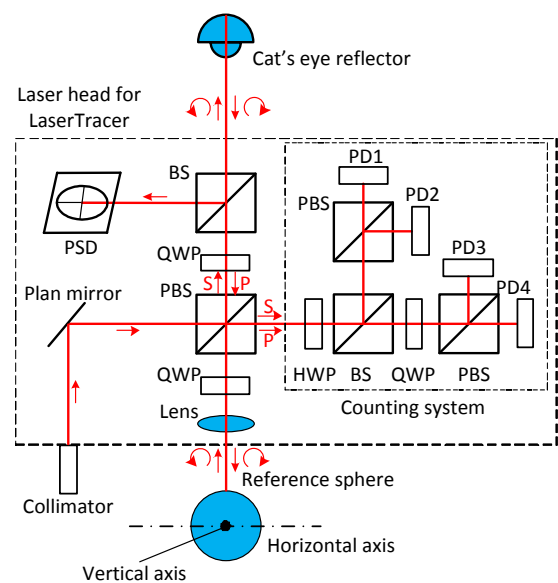


Fig.3. Optical system of LaserTracer.

### 2.1.1. Error motion along the vertical direction of measuring beam

As shown in Fig.1.a) and Fig.3., rotation error motions of gimbal mount axes in LaserTracer can be transmitted to laser head and all the optical components in laser head. The optical path of the reference beam remains unchanged during the measurement process and the outcome of laser interferometer depends on the variation of the optical path of the measuring beam. The optical path of the measuring beam is determined by the positions of the cat's eye reflector and the reference sphere. Although the positions of cat's eye reflector and reference sphere remain unchanged when the laser head and all optical components are driven by rotation errors of gimbal mount axes, it is not advisable to assume the unchanged optical path of the measuring beam. The focal point of lens deviates from the center of the reference sphere and may cause a certain amount of change of optical path because the lens is also driven by error motions. Therefore, it is necessary to explore the influences of the position variations of lens on measurement error of laser ranging. The complex optical system model of LaserTracer can be simplified because the optical path of the measuring beam in BS and QWPs remains unchanged. Therefore, we can easily explore the relationship between the position variation of optical components (cat's eye reflector, reference sphere, laser head, and measuring beam) and the outcome of laser interferometer.

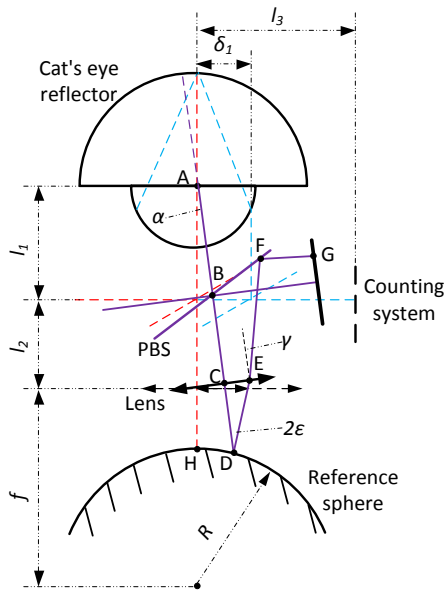


Fig.4. Optical path of measuring beam with error motion along the vertical direction of measuring beam in LaserTracer.

The position variation of measuring beam with the error motion along the vertical direction of measuring beam is shown in Fig.4.  $l_1$  is a variable representing the length between the cat's eye reflector and PBS.  $l_2=50$  mm represents the length between PBS and lens, and  $l_3=50$  mm represents the length between PBS and counting system. Both  $l_2$  and  $l_3$  are constants because all optical components are fixed inside the laser head.  $f=100$  mm represents the

focal length and the focal point coincides with the center of reference sphere.  $R=7.9378$  mm represents the radius of reference sphere.  $\delta_1=5$   $\mu\text{m}$  represents the offset of measuring beam caused by error motion along the vertical direction of the measuring beam. The values of  $l_2$ ,  $l_3$ ,  $f$ , and  $R$  are given according to the geometry of LaserTracer. It is difficult to precisely measure the geometric parameters of LaserTracer. Therefore, we choose the products of lens and reference sphere from Daheng Optics and HEXAGON. In the measurement process with LaserTracer, the measuring beam moves from red line to blue line. The blue line, which does not point to the center of the cat's eye reflector, will not point to the center of PSD either. Therefore, the signal of PSD controls two motors to ensure that the measuring beam points to the centers of the cat's eye reflector and PSD. Finally, the position of the measuring beam is changed to the purple line.  $\alpha$  represents the angle: between the theoretical position (red line without rotation errors) and the actual position (purple line with rotation errors) of the measuring beam.  $\epsilon$  represents the incident angle of the measuring beam on the surface of the reference sphere.  $\gamma$  represents the refraction angle of the measuring beam from the lens. Analysis and calculation results indicate the variation of optical path difference between the measuring beam and the reference beam is far less than 1 nm, irrespective of the refractive indices of all the crystals (see (1)).  $\Delta_{crystal}$  represents the variation of optical path difference before and after considering the refractive indices under the assumption that  $L_{crystal}=10$  cm is the total thickness of all the crystals of LaserTracer.  $n_{crystal}=1.5163$  represents the refractive index of K9.  $\gamma$  can be calculated according to (9). Therefore, the influences of refractive indices of all the crystals can be neglected. The actual optical path is  $l_{BA}+l_{AD}+l_{DE}+l_{EF}+l_{FG}$ . According to the geometric relationship shown in Fig.5. and Fig.6., we can calculate the optical path from the center of the cat's eye reflector to the surface of the reference sphere as well as the optical path from the surface of the reference sphere to the counting system.

$$\Delta_{crystal} = (n_{crystal} - 1) \cdot \frac{(1 - \cos \gamma)}{\cos \gamma} \cdot L_{crystal} = 0.17 \text{ nm} . \quad (1)$$

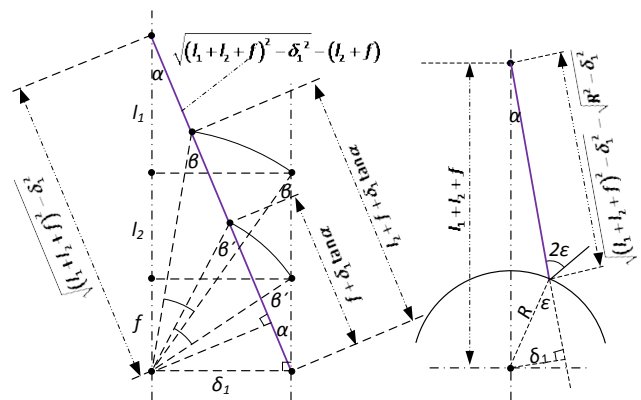


Fig.5. Measuring beam from the cat's eye reflector to the reference sphere.

The optical paths  $l_{BA}$  and  $l_{AD}$  are respectively given as (2) and (3):

$$l_{BA} = \sqrt{(l_1 + l_2 + f)^2 - \delta_1^2} - (l_2 + f); \quad (2)$$

$$l_{AD} = \sqrt{(l_1 + l_2 + f)^2 - \delta_1^2} - \sqrt{R^2 - \delta_1^2}. \quad (3)$$

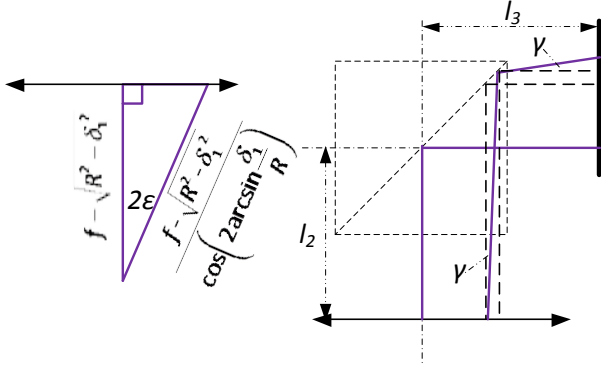


Fig.6. Measuring beam from the reference sphere to the counting system.

The angle between  $l_{CD}$  and  $l_{DE}$  is given as (4). The optical path  $l_{DE}$  is given as (5).

$$2\varepsilon = 2 \arcsin \frac{\delta_1}{R}; \quad (4)$$

$$l_{DE} = \frac{f - \sqrt{R^2 - \delta_1^2}}{\cos(2\varepsilon)}. \quad (5)$$

The parameters of biconvex lens are provided as follows.  $R_1=R_2=102.501$  mm represents the radii of biconvex lens;  $t=5$  mm represents the thickness of biconvex lens;  $n=1.5163$  represents the refractive index of biconvex lens.  $d_{in}$  and  $\theta_{in}$  represent the pose of beam  $l_{DE}$  and is given as (6) and (7):

$$d_{in} = \left( f - \sqrt{R^2 - \delta_1^2} \right) \cdot \tan(2\varepsilon); \quad (6)$$

$$\theta_{in} = 2\varepsilon. \quad (7)$$

According to ABCD matrix (8) and the pose of beam  $l_{DE}$ ,  $\gamma$  is calculated as (9):

$$\begin{bmatrix} d_{out} \\ \theta_{out} \end{bmatrix} = \begin{bmatrix} 1 & 0 \\ \frac{1-n}{R_1} & n \end{bmatrix} \cdot \begin{bmatrix} 1 & t \\ 0 & 1 \end{bmatrix} \cdot \begin{bmatrix} 1 & 0 \\ \frac{1-n}{nR_2} & \frac{1}{n} \end{bmatrix} \cdot \begin{bmatrix} d_{in} \\ \theta_{in} \end{bmatrix}; \quad (8)$$

$$\gamma = \theta_{out}. \quad (9)$$

The optical path  $l_{EF} + l_{FG}$  is given as (10):

$$l_{EF} + l_{FG} = \frac{l_2 + l_3}{\cos \gamma}. \quad (10)$$

The optical path difference of measuring beam without error motion along the vertical direction of measuring beam is given as (11):

$$\Delta_1 = 2(l_1 + l_2 + f - R). \quad (11)$$

The optical path difference of measuring beam with error motion along the vertical direction of measuring beam is given as (12):

$$\begin{aligned} \Delta_2 = & 2\sqrt{(l_1 + l_2 + f)^2 - \delta_1^2} - \sqrt{R^2 - \delta_1^2} - (l_2 + f) \\ & + \frac{f - \sqrt{R^2 - \delta_1^2}}{\cos 2\varepsilon} + \frac{l_2 + l_3}{\cos \gamma} - l_3. \end{aligned} \quad (12)$$

We can easily calculate the variation of optical path difference caused by error motion along the vertical direction of measuring beam, as in (13). According to (14), laser ranging measurement error is independent of the displacement between the center of the cat's eye reflector and PBS. According to (15), laser ranging measurement error is less than  $0.04 \mu\text{m}$  when error motion along the vertical direction of measuring beam is around  $\pm 5 \mu\text{m}$ :

$$\Delta_{12} = \Delta_2 - \Delta_1 = 2\sqrt{l_1^2 + 300l_1 + 22499.999975} - 2l_1 - 299.999923; \quad (13)$$

$$\frac{d\Delta_{12}}{dl_1} = -2 + \frac{2(150 + l_1)}{\sqrt{-0.000025 + (150 + l_1)^2}} = 0; \quad (14)$$

$$\begin{cases} \text{MaxValue}[\Delta_{12}] = 78 \text{ nm} \\ \text{MinValue}[\Delta_{12}] = 77 \text{ nm} \end{cases}. \quad (15)$$

### 2.1.2. Error motion along measuring beam

The position variation of the measuring beam with error motion along the direction of the measuring beam is shown in Fig.7.  $\delta_2=5 \mu\text{m}$  represents the offset of the measuring beam caused by error motion along the direction of the measuring beam. In the measurement process with LaserTracer, the position of measuring beam does not change. Only the focal point is changed by  $\delta_2$  along the direction of the measuring beam, thus changing the diameter of the reflected beam. On the contrary, the optical path difference of measuring beam remains unchanged with error motion along the direction of the measuring beam. Therefore, the laser ranging measurement accuracy is not affected by error motion along the direction of the measuring beam.

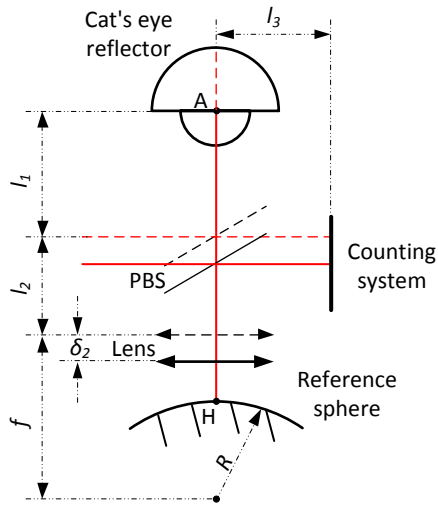


Fig.7. Optical path of measuring beam with error motion along the direction of measuring beam in LaserTracer.

2.2. Our simple model for LaserTracer

The positions of the cat's eye reflector and the reference sphere are fixed, whereas the positions of the measuring beam, PBS and lens are changed, as shown in Fig.4. However, it seems that all components except the reference sphere are fixed. In order to facilitate the experiment process for studying the influences of two types of error motions on the measurement accuracy of laser ranging, it is necessary to simplify the optical system model of LaserTracer. Based on the principle of relative motion, we design a simple optical system model (Fig.8.). Our model has three main advantages.

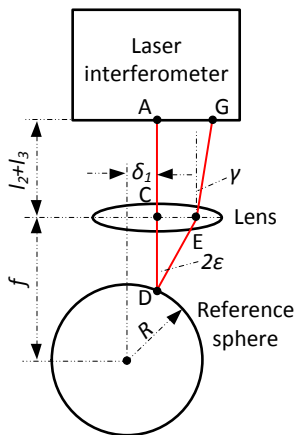


Fig.8. Simple optical system model for LaserTracer.

Firstly, it can use two movements to simulate 12 error motions in gimbal mount axes. Therefore, it is not necessary to build gimbal mount axes and the experimental cost and difficulty are reduced. Secondly, our model does not simulate rotatory movement and new rotation errors are not introduced. In the measurement process with LaserTracer, laser head needs a rotatory movement to make the laser beam point to the center of the cat's eye reflector and PSD. The position of the measuring beam is changed from the red

line to the purple line (see Fig.4.). In our model, all the error motions are realized by driving the reference sphere according to the principle of relative motion. Thirdly, fewer uncertainties are introduced into the model because few instruments are used. In order to replace the optical system model of LaserTracer correctly, the parameters in Fig.8. should be consistent with the parameters shown in Fig.4.

2.3. Experimental verification

In the verification experiments, error motions were simulated by driving the reference sphere with the precision positioning platform. Laser interferometer was fixed on a 3D slide table and finely adjusted to ensure laser beam parallels with the plan of optical platform (Fig.9.). A diaphragm was fixed between laser interferometer and biconvex lens. By adjusting the position of biconvex lens, the optical axis overlapped the laser beam. Diaphragm and biconvex lens were fixed near laser interferometer to diminish the dead path error. The precision positioning platform was firstly placed in the vicinity of the focal point of biconvex lens and the reference sphere was then fixed on the precision positioning platform. The position of reference sphere was finely adjusted to ensure that the reflected beam passed through the diaphragm and was irradiated in laser interferometer. Precision positioning platform moved along the red line, and the position of the reference sphere was regarded as the zero position when the outcome of laser interferometer was the lowest. At the same time, the center of reference sphere also overlapped the focal point of biconvex lens. The technical details of PI precision positioning platform are shown in Table 1.

Table 1. Details of PI precision positioning platform.

Model: P-561.3CD		Units
Travel	150 × 150 × 150	am
Resolution	0.2	nm
Positioning error	0.03	%
Repeatability	2	nm

The displacement between laser interferometer and lens is 100 mm, which equals the sum of l2 and l3. During the experiment, external adjusting devices were removed and not displayed in Fig.9.

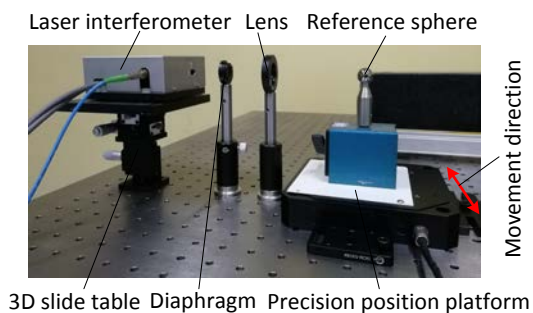


Fig.9. Experimental system for driving reference sphere along the vertical direction of laser beam.

### 3. RESULTS

Precision positioning platform moved 10  $\mu\text{m}$ , respectively, along the positive and negative directions with the step of 1  $\mu\text{m}$  and 4 groups of data of laser interferometer were recorded. The data of laser interferometer are shown in Table 2. The measurement data curves are shown in Fig.10. The mean curve represents the average value of 4 groups of data. Error bars represent the standard uncertainty ( $k=2$ ).

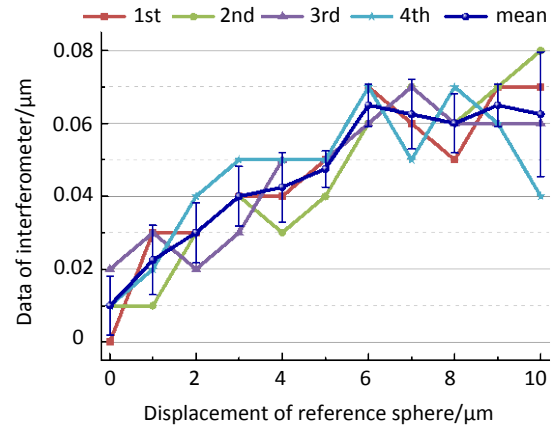
Table 2. Data of laser interferometer.

Error motion [ $\mu\text{m}$ ]	Outcome of laser interferometer [ $\mu\text{m}$ ]				Standard uncertainty [ $\mu\text{m}$ ]
	1st	2nd	3rd	4th	
0	0	0.01	0.02	0.01	0.01
1	0.03	0.01	0.03	0.02	0.01
2	0.03	0.03	0.02	0.04	0.01
3	0.04	0.04	0.03	0.05	0.01
4	0.04	0.03	0.05	0.05	0.01
5	0.05	0.04	0.05	0.05	0.01
6	0.07	0.06	0.06	0.07	0.01
7	0.06	0.07	0.07	0.05	0.01
8	0.05	0.06	0.06	0.07	0.01
9	0.07	0.07	0.06	0.06	0.01
10	0.07	0.08	0.07	0.04	0.02
0	0	-0.01	0	-0.01	0.01
-1	0.01	0	0.02	0.01	0.01
-2	0.02	0.01	0.03	0.02	0.01
-3	0.02	0.01	0.04	0.03	0.01
-4	0.04	0.02	0.03	0.02	0.01
-5	0.04	0.04	0.04	0.03	0.01
-6	0.05	0.05	0.04	0.03	0.01
-7	0.06	0.04	0.04	0.05	0.01
-8	0.05	0.02	0.06	0.04	0.02
-9	0.06	0.04	0.04	0.05	0.01
-10	0.07	0.05	0.05	0.04	0.01

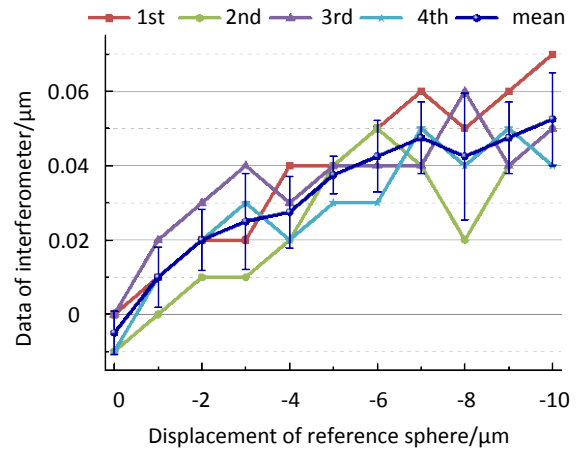
The standard deviation of results is calculated in (16) and shown in Table 2. Standard uncertainty caused by repeatability of measurement is given as (17) where ( $k=2$ ).  $n'$  represents the measurement times at the same error motion.  $l_i$  represents the  $i_{th}$  data of laser interferometer.

$$\sigma = \sqrt{\frac{\sum_{i=1}^{n'} (l_i - \bar{l})^2}{n' - 1}}; \quad (16)$$

$$u = k \cdot \frac{\sigma}{\sqrt{n'}}. \quad (17)$$



a) Positive direction.



b) Negative direction.

Fig.10. Experimental results of driving reference sphere along the vertical direction of laser beam.

When error motion along the positive direction is less than 5  $\mu\text{m}$ , the maximum laser ranging measurement error is 0.05  $\mu\text{m}$ ; when error motion along the negative direction is less than -5  $\mu\text{m}$ , the maximum laser ranging measurement error is 0.04  $\mu\text{m}$ . According to the above theoretical analysis, when error motion is  $\pm 5 \mu\text{m}$ , the maximum laser ranging measurement error is 0.04  $\mu\text{m}$ , which is consistent with the experimental result. The laser ranging measurement error still climbs to 0.08  $\mu\text{m}$  when error motion increases to 10  $\mu\text{m}$ . Both measuring result and error trend are consistent with the theoretical analysis, indicating that our simple model can replace the complex model of LaserTracer correctly. Moreover, theoretical and experimental data have verified that the spherical mirror of the laser tracking system can decrease the influences of rotation errors of gimbal mount axes.

### 4. DISCUSSION & CONCLUSIONS

In Fig.10., the data measured along the positive direction are slightly larger than those measured along the negative direction. The reason is that zero positions for positive and negative directions do not overlap well with each other.

According to theoretical and experimental result, error motion should be controlled within  $\pm 20 \mu\text{m}$ . When error motion is more than  $\pm 20 \mu\text{m}$ , the reflected beam is away from the cat's eye reflector or PSD, thus resulting in the separation of measuring beam and reference beam.

There are two reasons causing the little difference between theory and experiment in laser ranging measurement error. In Fig.4., error motion is a composite motion involving the main horizontal component and a tiny vertical component. PI precision positioning platform might be not extremely accurate. In the field of ultra-precision measurement, any tiny variation in the system might lead to inaccurate measurement results.

The analysis method and experiment scheme in this paper confirm that the spherical mirror of the laser tracking system can decrease the influences of rotation errors of gimbals mount axes on the measurement accuracy. Laser ranging measurement error caused by rotation errors is less than  $0.1 \mu\text{m}$  if rotation error motions are within  $\pm 10 \mu\text{m}$ . The results might be utilized to reduce the cost and the design requirements of the laser tracking system. Furthermore, studying the structure, which can decrease the influences of rotation errors in the readings of sensors, would be conducive to develop the research for form errors of cylindrical parts.

#### ACKNOWLEDGMENT

The work was supported by Beijing Municipal Science and Technology Commission [Z161100001516003], and National Key Scientific Instrument and Equipment Development Project of China [No.2013YQ17053904].

#### REFERENCES

- [1] Harding, H. (2013). *Handbook of Optical Dimensional Metrology*. CRC Press, Vol. 3, 95-104.
- [2] Schneider, C.T. (2004). LaserTracer – A new type of self tracking laser interferometer. In *8th International Workshop on Accelerator Alignment*, 4-7 October 2004. Geneva, Switzerland : European Laboratory for Particle Physics, 1-6.
- [3] Peggs, G.N., Maropoulos, P.G., Hughes, E.B., Forbes, A.B., Robson, S., Ziebart, M., Muralikrishnan, B. (2009). Recent developments in large-scale dimensional metrology. *Proceedings of the Institution of Mechanical Engineers, Part B: Journal of Engineering Manufacture*, 223 (6), 571-595.
- [4] Schwenke, H., Schmitt, R., Jatzkowski, P., Warmann, C. (2009). On-the-fly calibration of linear and rotary axes of machine tools and CMMs using a tracking interferometer. *CIRP Annals - Manufacturing Technology*, 58, 477-480.
- [5] Schwenke, H., Franke, M., Hannaford, J., Kunzmann, H. (2005). Error mapping of CMMs and machine tools by a single tracking interferometer. *CIRP Annals - Manufacturing Technology*, 54, 475-478.
- [6] Camboulives, M., Lartigue, C., Bourdet, P., Salgado, J. (2016). Calibration of a 3D working space by multilateration. *Precision Engineering*, 44, 163-170.
- [7] Gaska, A., Sladek, J., Ostrowska, K., Kupiec, R., Krawczyk, M., Harmatys, W., Gaska, P., Gruza, M., Owczarek, D., Knapik, R., Kmita, A. (2015). Analysis of changes in coordinate measuring machines accuracy made by different nodes density in geometrical errors correction matrix. *Measurement*, 68, 155-163.
- [8] Muralikrishnan, B., Lee, V., Blackburn, C., Sawyer, D., Phillips, S., Ren, W., Hughes, B. (2013). Assessing ranging errors as a function of azimuth in laser trackers and tracers. *Measurement Science and Technology*, 24, 065201.
- [9] Muralikrishnan, B., Phillips, S., Sawyer, D. (2016). Laser trackers for large-scale dimensional metrology: A review. *Precision Engineering*, 44, 13-28.
- [10] Hughes, B., Forbes, A., Lewis, A., Sun, W.J., Veal, D., Nasr, K. (2011). Laser tracker error determination using a network measurement. *Measurement Science and Technology*, 22, 045103.
- [11] Feng, D.Y., Gao, Y.G., Zhang, W.B. (2011). Elimination of shafting errors in photoelectrical theodolites with standard-bearings. *Optics and Precision Engineering*, 19, 605-611.
- [12] Conte, J., Majarena, A.C., Acero, R., Santolaria, J., Aguilar, J.J. (2015). Performance evaluation of laser tracker kinematic models and parameter identification. *The International Journal of Advanced Manufacturing Technology*, 77, 1353-1364.
- [13] Acero, R., Santolaria, J., Pueo, M., Brau, A. (2016). Real-time laser tracker compensation of a 3-axis positioning system-dynamic accuracy characterization. *The International Journal of Advanced Manufacturing Technology*, 84, 595-606.
- [14] Lee, H.W., Chen, J.R., Pan, S.P., Liou, H.C., Hsu, P.E. (2016). Relationship between ISO 230-2/-6 test results and positioning accuracy of machine tools using LaserTRACER. *Applied Sciences*, 6, 105.
- [15] International Organization for Standardization. (2006). *Test code for machine tools - Part 7: Geometric accuracy of axes of rotation*. ISO 230-7:2006.
- [16] Zhao, J.T., Hu, X.D., Zou, J., Zhao, G.Y., Lv, H.Y., Xu, L.Y., Xu, Y., Hu, X.T. (2016). Method for correction of rotation errors in Micro-CT System. *Nuclear Instruments and Methods in Physics Research A*, 816, 149-159.

Received September 11, 2017.

Accepted January 29, 2018.